Geosci. Model Dev. Discuss., 7, 1413–1452, 2014
www.geosci-model-dev-discuss.net/7/1413/2014/
doi:10.5194/gmdd-7-1413-2014

Geoscientific Model Development
Discussions
Open Access

Analysing Amazonian forest productivity using a new individual and trait-based model (TFS v.1)

N. M. Fyllas[1,*], E. Gloor[1], L. M. Mercado[2], S. Sitch[2], C. A. Quesada[3], T. F. Domingues[4], D. R. Galbraith[1], A. Torre-Lezama[5], E. Vilanova[5], H. Ramírez-Angulo[5], N. Higuchi[3], D. A. Neill[6], M. Silveira[7], L. Ferreira[8], G. A. Aymard C[9], Y. Malhi[10], O. L. Phillips[1], and J. Lloyd[11,12]

[1]Ecology and Global Change, School of Geography, University of Leeds, Leeds, UK
[2]School of Geography, University of Exeter, Exeter, UK
[3]Instituto Nacional de Pesquisas da Amazônia, Manaus, Brazil
[4]School of GeoSciences, University of Edinburgh, Edinburgh, Scotland, UK
[5]Instituto de Investigaciones para el Desarrollo, Forestal Facultad de Ciencias Forestales y Ambientales, Universidad de Los Andes, Mérida, Venezuela
[6]Department of Wildlife Conservation and Management, Universidad Estatal Amazónica, Puyo, Pastaza, Ecuador
[7]Universidade Federal do Acre, Rio Branco, Brazil
[8]Museu Paraense Emílio Goeldi, Belém, Brazil

[9]UNELLEZ (Universidad Nacional Experimental de los Llanos Occidentales Ezekiel Zamora) – Guanare, Programa de Ciencias del Agro y el Mar, Herbario Universitario (PORT), estado Portugesa, Venezuela
[10]Environmental Change Institute, School of Geography and the Environment, University of Oxford, Oxford, UK
[11]Centre for Tropical Environmental and Sustainability Science (TESS) and School of Marine and Tropical Biology, James Cook University, Cairns, Australia
[12]Department of Life Sciences, Imperial College London, Silwood Park Campus, Ascot, UK
[*]now at: Department of Ecology and Systematics, Faculty of Biology, University of Athens, Athens, Greece

Received: 24 January 2014 – Accepted: 4 February 2014 – Published: 20 February 2014

Correspondence to: N. M. Fyllas (nfyllas@gmail.com)

Published by Copernicus Publications on behalf of the European Geosciences Union.

Abstract

Repeated long-term censuses have revealed large-scale spatial patterns in Amazon Basin forest structure and dynamism, with some forests in the west of the Basin having up to a twice as high rate of aboveground biomass production and tree recruitment as forests in the east. Possible causes for this variation could be the climatic and edaphic gradients across the Basin and/or the spatial distribution of tree species composition. To help understand causes of this variation a new individual-based model of tropical forest growth designed to take full advantage of the forest census data available from the Amazonian Forest Inventory Network (RAINFOR) has been developed. The model incorporates variations in tree size distribution, functional traits and soil physical properties and runs at the stand level with four functional traits, leaf dry mass per area (M_a), leaf nitrogen (N_L) and phosphorus (P_L) content and wood density (D_W) used to represent a continuum of plant strategies found in tropical forests. We first applied the model to validate canopy-level water fluxes at three Amazon eddy flux sites. For all three sites the canopy-level water fluxes were adequately simulated. We then applied the model at seven plots, where intensive measurements of carbon allocation are available. Tree-by-tree multi-annual growth rates generally agreed well with observations for small trees, but with deviations identified for large trees. At the stand-level, simulations at 40 plots were used to explore the influence of climate and soil fertility on the gross (Π_G) and net (Π_N) primary production rates as well as the carbon use efficiency (C_U). Simulated Π_G, Π_N and C_U were not associated with temperature. However all three measures of stand level productivity were positively related to annual precipitation and soil fertility.

1 Introduction

The Amazon Basin encompasses one of the planet's largest forest areas, hosting one quarter of the Earth's biodiversity and constitutes a large reservoir of living biomass (Malhi and Phillips, 2005). Amazon forests also have a substantial influence on regional and global climates (Shukla et al., 1990; Spracklen et al., 2012). These forests are, however, under strong human pressure through logging, forest to pasture conversion, and face at present a warming and more variable climate and changing atmospheric composition (Lewis et al., 2004; Gloor et al., 2013). Due to the enormous area of forest within the Amazon Basin, these factors have the potential to modify global atmospheric greenhouse concentrations, regional and global climate, and the overall biodiversity of the planet (Cramer et al., 2004).

Traditionally, two approaches have been followed to understand current and future state of the Amazon forests. First, Dynamic Global Vegetation Models (DGVM) have been used to simulate vegetation patterns and carbon fluxes across Amazonia (Moorcroft et al., 2001; Galbraith et al., 2010) with some predicting substantial carbon losses under scenarios of global change (White et al., 1999; Cox et al., 2004) but with others less so (Cramer et al., 2004), or even gains (Huntingford et al., 2013). A second approach to understand Amazonian forests dynamics is through the analysis of long-term field observations of patterns of tree growth and mortality as they relate to climatic and edaphic variations across the Basin (e.g. Phillips et al., 2004; Quesada et al., 2012).

Analyses of Amazon forest inventory data, and particularly those of the Amazon Forest Inventory Network (RAINFOR) (Malhi et al., 2002), have revealed large-scale temporal trends in biomass and species composition as well as intriguing spatial patterns in many stand properties (Phillips et al., 1998, 2009; Baker et al., 2004). Specifically, there is systematic spatial variation in species composition, biomass, growth and turnover rates, with western forests exhibiting higher wood productivity, faster turnover time and lower stand wood density compared to eastern forests (Baker et al., 2004; Malhi et al., 2006). This macroecological variation may possibly be explained by the Basin-wide observed climate and soil fertility gradients (Ter Steege et al., 2006; Quesada et al., 2012). The climatic gradient comprises a southeast to northwest increase in annual precipitation and decrease in dry season length (Sombroek, 2001), with aboveground wood productivity positively related to precipitation (Malhi et al., 2004). On the other hand, a soil age/fertility axis spans from the northeastern part of the basin to southwestern

Amazonia, with generally younger and richer soils in the west and highly weathered nutrient poor soils in the east (Sombroek, 2000; Quesada et al., 2011), although at regional and local scales the patterns are often more complicated than this macro-gradient might imply (Higgins et al., 2011). Soil physical properties (such as rooting depth, drainage and water holding capacity and soil structure) are similarly related to soil age and parental material (Quesada et al., 2010). Poor physical (for example soil depth) conditions (less weathered soils) are associated with higher soil fertility (Walker and Syers, 1976; Vitousek and Farrington, 1997) leading to increased nutrient concentrations at the leaf level (Fyllas et al., 2009) and thus a potential for higher photosynthetic rates (Reich et al., 1994; Raaimakers et al., 1995). In addition, increased disturbance-associated mortality rates in soils of poor physical properties appear to lead to more dynamic stands where faster growing species dominate (Chao et al., 2009; Quesada et al., 2012). This could explain the higher aboveground productivity observed for western forests, through a positive feedback mechanism (Quesada et al., 2012).

The simplistic ways by which plant functional diversity is currently reflected in DGVMs is an important shortcoming in predicting ecosystem response to environmental gradients and their vulnerability to global change (Lavorel et al., 2007). Some of the widely applied DGVMs represent Amazonian plant diversity with only few plant functional types (PFT), for example the LPJ model uses only two tropical-oriented PFTs (Sitch et al., 2003) and the JULES model only one (Clark et al., 2011). The mean values of key model parameters like photosynthetic capacity, wood density and leaf turnover times are selected to describe an a priori PFT definition (Fyllas et al., 2012). This means that many processes are controlled by a set of fixed parameters that describe viable plant strategies within very limited boundaries. Such PFT implementation has important drawbacks. It is usually based on the average value of a plant trait recorded from different field studies and different species. But recent studies have shown that key traits present a wide variation, dependent upon species identity and site growing conditions (Sultan, 2000; Fyllas et al., 2009; Baraloto et al., 2010a). Thus any given species has the potential to exhibit site-dependent shifts in its trait value, in addition to the interspecific trait variability found at any given site. Ignoring this plasticity could potentially bias modelling through an underestimation of the PFT's resilience by projecting dramatic but artificial switches in vegetation state caused by the limited and discrete (step-wise) nature of PFT descriptions.

Such unaccounted variability could be particularly important when modelling Amazonian forest dynamics, where environmental heterogeneity and plant functional diversity comprise key components of the ecosystem (Townsend et al., 2008). For example, the variation in leaf mass per area (M_a) recorded within Amazon forests covers an approximately similar range to the one identified in global datasets, ranging from 30 to 300 $\mathrm{g\,m^{-2}}$ (Fyllas et al., 2009). Similarly, there is large variation in forest physical and chemical conditions (Quesada et al., 2010). These two important ecosystem components have now been better quantified with Amazon-wide climate (Malhi and Wright, 2004), soil (Quesada et al., 2011) and functional trait datasets having been obtained (Baker et al., 2009; Fyllas et al., 2009; Patiño et al., 2009, 2012). This is in addition to continually expanding long-term forest inventory data in which tree growth, mortality and species composition data are regularly being recorded (Keeling et al., 2008; Chao et al., 2009).

We here introduce a vegetation dynamics model specifically designed to account for these environmental and the biotic variations as a tool to better analyse observed Amazonian large-scale patterns. Specifically we focus (a) on the architectural variability, expressed through the size-class distribution of a stand, and (b) on the functional variability, expressed through the distribution of four important functional traits, both within and among forest plots. Following a continuum approach, we replace the use of a discrete number of PFTs, with distributions of a functional traits "quartet".

Two functional dimensions are represented in the model: the leaf economic and the tree architecture spectra. The four functional traits include leaf mass per area (M_a), leaf N and P dry mass concentration (N_{Lm} and P_{Lm} respectively) and wood density (D_W). The first three traits express one component of the leaf economic spectrum (Reich et al., 1997; Wright et al., 2004), i.e. a global photosynthetic tissue trade-off between inexpensive, short-lived and fast payback leaves vs. costly, long-lived and slow payback leaves; although we emphasise that other factors such as leaf cation concentrations may be important in this respect (Fyllas et al., 2012; Patiño et al., 2012). Low M_a and high nutrient content leaves are associated with comparably short longevity. Co-varying with M_a are usually $\mathrm{N_{Lm}}$ and $\mathrm{P_{Lm}}$, with low M_a leaves usually having higher nutrient concentrations and thus supporting higher (mass-based) gas exchange rates (Reich et al., 1994; Raaimakers et al., 1995). Lately the role of $\mathrm{P_{Lm}}$ has been highlighted as it expresses alternative limitations of the photosynthetic efficiency of tropical tree species (Domingues et al., 2010). The fourth trait, D_W, is used to represent a tree architectural dimension with denser wood species supporting an overall higher aboveground biomass and thus having a higher maintenance respiration (Chave et al., 2005; Mori et al., 2010, although see Larjavaara and Muller-Landau, 2012). These two dimensions capture essentially a growth vs. survival trade-off. There is mixed evidence for a coordination between leaf and stem traits, i.e. a correlation between slow return related leaf traits and denser wood (Chave et al., 2009), with Baraloto et al. (2010b) suggesting that these two axes are independent, but with Patiño et al. (2012) showing some important correlations with foliar traits such as $\mathrm{P_{Lm}}$. For the purpose of this study we consider leaf and stem dimensions as independent axes of tree functional variation, with no predefined interrelationship between the representative traits. However, the observed among-stand variability of these four characters is used to express how growing conditions control plant processes while the within-stand trait variation represents a range of ecological strategies found under the same growing conditions.

The model is initialised with site-specific tree diameter and functional traits data, and forced with daily climate data. We first test the ability of the model to estimate stand-level water fluxes at three eddy-flux tower sites. For a subset of seven RAINFOR plots where site-specific carbon allocation coefficients are known, a tree-level test of stem growth rates is applied. We further validate the ability of the model to simulate the spatial patterns of aboveground biomass productivity at 40 RAINFOR plots, and subsequently explore the variation of Gross Primary Productivity (Π_G), Net Primary Productivity (Π_N) and Carbon Use Efficiency (C_U) along established Amazonian climatic and edaphic gradients.

2 Materials and methods

2.1 Model description

"Traits-based Forest Simulator" (TFS) is an individual-based forest model, i.e. it simulates water and carbon fluxes for each tree in a stand. In the current version of the model, stand structure is prescribed in terms of the number of trees and their diameter at breast height (d). In this study a "snapshot" version of the model is used which does not take into account tree recruitment and mortality. An individual is fully described through d, with allometric equations used to estimate other attributes of interest like tree height (H), crown area (C_A), total leaf area (L_A) and tree-level leaf area index (L). Whole tree biomass is partitioned to leaf (B_L), stem (B_S), coarse root (B_{C_R}) and fine root (B_{FR}) biomass, based on allometric equations. The general architecture of the model is presented in Fig. 1.

The functional diversity of the trees in a stand is expressed through four traits (M_a, N_{Lm}, P_{Lm}, D_W) randomly assigned from local observations, using a data-driven random vector generation algorithm. Leaf photosynthesis is calculated using the Farquhar biochemical model (Farquhar et al., 1980) with a modification of the total air-to-chloroplast conductance to be regulated by the soil moisture concentration. Hourly carbon and daily water fluxes are estimated for each tree, while light competition is based on the assumption of a perfect canopy tessellation and flat disc-shaped canopies. This simple tree architecture simplifies the way light competition is approximated, by identifying canopy and sub-canopy trees based on the tessellation process and tree height distribution (Purves et al., 2007). Soil water balance is approximated through a simple bucket model, with soil water content and vapour pressure deficit regulating leaf conductance. Allocation of assimilated carbon to different plant components is static, i.e. it does not change with size or resource availability, but rather implements field-derived allocation coefficients (Aragão et al., 2009).

TFS is coded in Java and it is fully described in Sect. S1. Model components that are particularly developed for this analysis are presented in the following paragraphs. All statistical analyses and graphs were made with R (R Development Core Team, 2013).

2.1.1 Initialisation and within stand functional diversity

As noted above, TFS employs neither species nor PFT descriptions, but rather continua of the four key functional traits M_a, N_{Lm}, P_{Lm} and D_W used to characterize an individual tree along with a d-based allometry. These functional characters are assigned to individual trees based on observed plot-level data and using a random vector generation algorithm (Taylor and Thompson, 1986). This algorithm is appropriate for generating non-repeated pseudo-observations from a relatively small sample of observations. In our case, coordinated trait suites for each tree in a stand are generated based on a smaller trait sample from trees in the same stand. This initialisation approach ensures that within stand functional variation and trait covariances are preserved without any assumptions having to be made about their underlying statistical distributions. Thus no single functional trait "average stand" value is used. Further, between-stand differences in the traits distributions and their covariances that may have arisen from either the successional status or the growing conditions of the stand are also taken into account. This is because each stand is characterised by its own multivariate trait sample and size distribution. More fertile plots have an overall lower M_a and higher N_{Lm} and P_{Lm} compared to infertile plots (Fyllas et al., 2009), with this being reflected in the photosynthetic capacity of individual trees, as described in the next paragraph.

2.1.2 Light interception and carbon assimilation

The "flat top" version of the perfect plasticity model (Purves et al., 2007) is used to specify if a tree is at the canopy or sub-canopy level. Radiation absorption is then estimated by assuming that canopy trees intercept direct, diffuse and scattered radiation, while sub-canopy trees intercept only diffuse and scattered radiation, in correspondence with the sun-shade implementation of the Farquhar model (de Pury and Farquhar, 1997; Wang and Leuning, 1998). A tree-level leaf area index (L), estimated as the ratio of L_A to C_A, is used to compute the energy, carbon and water fluxes for each tree in a stand. The net photosynthetic rate ($\mu\mathrm{mol\,m^{-2}\,s^{-1}}$) is given from:

$$A_n = g_\mathrm{s}(C_\alpha - C_\mathrm{c}) \tag{1}$$

with C_α the atmospheric CO$_2$ mixing ratio ($\mu\mathrm{mol\,mol^{-1}}$), C_c the CO$_2$ mixing ratio inside the chloroplast and g_s the CO$_2$ stomatal conductance ($\mathrm{mol\,m^{-2}\,s^{-1}}$) calculated from Medlyn et al. (2011) and modulated by a soil moisture term (see also stomatal conductance paragraph). The leaf-level photosynthetic rate A_n is scaled-up to the tree-level by multiplying with the C_A of the tree.

2.1.3 Photosynthesis and respiration

Here we implement the co-limitation equation suggested by Domingues et al. (2010), where the leaf level photosynthetic capacity (area basis) is potentially limited by either nitrogen or phosphorus concentrations according to:

$$V_\mathrm{max} = M_\mathrm{a}(\min\{a_\mathrm{NV} + v_\mathrm{NV}\mathrm{N_{Lm}}, a_\mathrm{PV} + v_\mathrm{PV}\mathrm{P_{Lm}}\}) \tag{2}$$

$$J_\mathrm{max} = M_\mathrm{a}(\min\{a_\mathrm{NJ} + v_\mathrm{NJ}\mathrm{N_{Lm}}, a_\mathrm{PJ} + v_\mathrm{PJ}\mathrm{P_{Lm}}\}) \tag{3}$$

both in ($\mu\mathrm{mol\,m^{-2}\,s^{-1}}$), and a_NV, a_NJ, a_PV, a_PJ in ($\mu\mathrm{mol\,g^{-1}\,s^{-1}}$) and v_NV, v_NJ, v_PV, v_PJ in ($\mu\mathrm{mol\,mg^{-1}\,s^{-1}}$) empirical coefficients (see Sect. S1).

Title Page
Abstract | Introduction
Conclusions | References
Tables | Figures
◀| |▶
◀ ▶
Back | Close
Full Screen / Esc
Printer-friendly Version
Interactive Discussion

The canopy-level photosynthetic capacity V_{Cmax} (μmol m^{-2} s^{-1}) is estimated using the tree-level leaf area index L, taking into account within canopy gradients in light and photosynthetic capacity based on Lloyd et al. (2010). The modified Farquhar photosynthesis model then computes hourly CO$_2$ assimilation as described in Sect. S1. Nutrient optimisation is approximated using the equation of Lloyd et al. (2010) with M_{a} also dependent on the height of each tree.

Tree respiration includes a growth and a maintenance component, both computed daily. Growth respiration is considered as a constant fraction (0.25) of daily photosynthesis (Cannell and Thornley, 2000). Three different maintenance respiration formulations are allowed in TFS (Sect. S1), but in this study we use the formulation below. Leaf maintenance respiration R_{mL} is estimated as a fraction of V_{Cmax} (Scheiter and Higgins, 2009):

$$R_{\mathrm{mL}} = 0.015 V_{\mathrm{Cmax}} \tag{4}$$

Stem maintenance respiration is estimated from the sapwood volume (V_{S}) of a tree:

$$R_{\mathrm{mS}} = \delta V_{\mathrm{S}} \tag{5}$$

with $\delta = 39.6$ (μmol m^{-3} s^{-1}) as reported in Ryan et al. (1994) for tropical trees.

Coarse root maintenance respiration R_{mCR} is estimated as in Scheiter and Higgins (2009):

$$R_{\mathrm{mCR}} = 0.218 \beta_{\mathrm{R}} \frac{B_{\mathrm{CR}}}{\Phi_{\mathrm{CN}}} \tag{6}$$

where Φ_{CN} is the root C : N ratio estimated on the basis of the simulated N_{R} assuming a dry weight carbon fraction of 0.5.

Fine root maintenance respiration R_{mFR} is assumed to be equal to leaf respiration.

All respiratory components are corrected with the temperature dependence function of Tjoelker et al. (2001). The total maintenance respiration R_{m} is then:

$$R_{\mathrm{m}} = R_{\mathrm{mL}} + R_{\mathrm{mS}} + R_{\mathrm{mCR}} + R_{\mathrm{mFR}} \tag{7}$$

2.1.4 Stomatal conductance

Initially, a maximum (no water stress) stomatal conductance, $g_{\mathrm{s,max}}$ is calculated following Medlyn et al. (2011, 2012):

$$g_{\mathrm{s,max}} = g_0 + 1.6 \cdot \left(1 + \frac{g_1}{\sqrt{D_{\mathrm{C}}}}\right) \times \frac{A_n}{C_{\mathrm{a}}} \tag{8}$$

with g_0 ($\mathrm{mol\,m^{-2}\,s^{-1}}$) the minimum stomatal conductance, g_1 (–) an empirical coefficient that represents the water use efficiency of the plant, and D_{C} the leaf-to-atmosphere vapour pressure difference. Values of g_0 and g_1 that lead to the best model performance were different between sites, as indicated by the model calibration procedure. For the basin-wide simulations constant values of $g_0 = 0.020$ ($\mathrm{mol\,m^{-2}\,s^{-1}}$) and $g_1 = 5.0$ (–) were used, close to the estimates of Domingues et al. (2013). In future versions of the model, we anticipate that g_0 and g_1 will be related to other functional traits. The maximum stomatal conductance is subsequently reduced to the actual g_{S} by multiplying the second term of Eq. (8) with a water stress coefficient described in the next paragraph.

2.1.5 Soil water balance and water availability effects on stomatal conductance

A single-layer soil bucket model is used in the current version of the model to estimate soil water content and the down-regulation of stomatal opening in case of limited soil water. We are aware that this is a component that needs further improvement in the future but for the purpose of this study which is to explore to first order the basic functioning of forest stand carbon uptake and water loss a single-layer soil model should be sufficient. In contrast to most ecosystem fluxes model, where photosynthetic rates are directly regulated by water availability (Cox et al., 1998; Clark et al., 2011), we couple soil water deficits to canopy conductances by estimating a daily fractional available soil water content ϑ_i, for the i-th tree in the stand given from:

$$\vartheta_i = \frac{W_i - W_\mathrm{W}}{W_\mathrm{FC} - W_\mathrm{W}} \tag{9}$$

where W_i the available water for tree i, W_FC is the soil water content at field capacity (matric potential of 0.033 MPa) and W_W is the soil water content at wilting (matric potential of 1.5 MPa), both estimated using the van Genuchten (1980) model with the soil-type specific parameters reported in Hodnett and Tomasella (2002).

The estimation of W_i at time t is given from (see Sect. S1 for details):

$$W_{i,t} = W_{t-1} + (P_t - E_{\mathrm{tot},t} - Q_t) + Z_{\mathrm{R},i} - Z_\mathrm{D} \tag{10}$$

Here W_{t-1} is the previous day's (stand level) soil water column, P_t is the daily total precipitation, $E_{\mathrm{tot},t}$ the daily total (stand level) evaporation, Q_t the run-off, $Z_{\mathrm{R},i}$ is the root depth of tree i, and Z_D the soil depth all expressed in mm. The rooting depth of each tree is estimated in a similar way to Scheiter and Higgins (2009), as the biomass needed to construct a root cylinder of radius R_r ($R_\mathrm{r} = 0.15\,\mathrm{m}$) with a density D_r ($D_\mathrm{r} = 100\,\mathrm{kg\,m^{-3}}$):

$$Z_\mathrm{R} = \frac{B_\mathrm{FR}}{\pi D_\mathrm{r} R_\mathrm{r}^2} \tag{11}$$

A tree specific water stress term γ_i that has a direct effect on stomatal conductance (as a multiplier) is subsequently estimated from:

$$\gamma_i = \vartheta_i^n \tag{12}$$

As discussed in Keenan et al. (2010) the exponent in Eq. (12), is a measure of the non-linearity of the effects of soil water stress on stomatal conductance. The smaller the value of n, the less sensitive is canopy conductance to soil water stress. In our case we found a value of $n = 0.25$ to give best agreement with observations in regards to the response of stomatal conductance to changes in water availability and the long-term simulation of carbon fluxes.

2.2 Study sites and simulations set-up

Three sets of site data were used to explore the behaviour of the model. These include a set of three eddy flux measurements (EFM) sites, seven plots with intensive carbon balance and allocation measurements (IM), and 40 permanent measurement plots (PM).

2.2.1 Eddy flux (EFM) sites

Daily climate and energy flux data from three EFM sites (Caxiuanã [1.72° S, 51.46° W], Manaus [2.61° S, 60.21° W] and Tapajós [2.86° S, 54.96° W]) were used to assess the ability of the model to estimate canopy-level water fluxes. Data were obtained from the Large Scale Biosphere–Atmosphere Experiment in Amazonia (LBA) project (http://daac.ornl.gov/LBA/lba.shtml). In particular mean daily climate parameters including incoming radiation, temperature, precipitation, relative humidity and wind speed were used to force the model. Latent heat flux (λE in $\mathrm{W\,m^{-2}}$) was used to estimate a daily mean canopy conductance defined as $G_\mathrm{C} = \frac{\lambda E}{D_\mathrm{C}}$. The EFM data cover a period from 2001 to 2008 for Caxiuanã, from 2000 to 2005 for Manaus and from 2002 to 2004 for Tapajós. G_C was only estimated for days with a complete diurnal record of λE. At each one of the EFM sites the mean daily G_C ($\mathrm{mol\,m^{-2}\,s^{-1}}$) was compared between observations and simulations. The model was initialized with size-class distribution and functional traits data from RAINFOR permanent plots located near the eddy flux towers. In particular CAX-06 inventory data were used for Caxiuanã, BNT-04 for Manaus, and TAP-55 for Tapajós. We note that the EFM sites are mainly found at the eastern part of Amazonia (Fig. 2) growing on low fertility soils.

The model was initially calibrated to the site specific values for g_0 and g_1 of Eq. (8) that gave the best performance. A Standardised Major Axis (SMA) regression, forced through zero was used to verify the ability of the model to simulate G_C, with a regression slope close to one indicating a good model performance.

2.2.2 Intensive measurement (IM) sites

The ability of the model to realistically simulate carbon fluxes at the tree-level is evaluated using data from the seven intensive measurement plots (Aragão et al., 2009; Malhi et al., 2009). These sites are amongst the intensively surveyed plots within the RAINFOR network (Fig. 2), where measurements of all major components of the C cycle are recorded (Malhi et al., 2009). At these plots, a detailed assessment of the carbon stocks is applied, and Π_N allocation coefficients to different plant components are estimated (Aragão et al., 2009; Malhi et al., 2011; Doughty et al., 2013). These site-specific coefficients are used to calculate the amount of simulated Π_N that is allocated to stems $\Pi_{N,s}$ ($\mathrm{kg\,C\,yr^{-1}}$).

The IM sites of interest include two plots at Agua Pudre in Colombia (AGP-01 and AGP-02), one (ALP-30) at Allpahuayo/Peru, one (BNT-04) at Manaus/Brazil, one in Caxiuanã/Brazil (CAX-06), one in Tambopata/Peru (TAM-05) and one in (TAP-55) Tapajós/Brazil. Based on data from Quesada et al. (2011), AGP-01, AGP-02, TAM-05 can be considered to be located on fertile soils, with the other four plots on infertile ones. Available soil depth data (Quesada et al., 2011) and functional traits data (Fyllas et al., 2009) were used for site specific simulations. For all seven sites we estimated the observed average multi-annual growth rate (2000–2006) of each tree from forest census data, in order to compare it with the simulated $\Pi_{N,s}$.

The daily climate was extracted from the Princeton Global Meteorological Forcing Dataset (Sheffield et al., 2006). These simulations are used to validate the ability of the model to accurately estimate tree-level stem growth, under a given stand structure, a given climatic and soil profile and functional traits configuration of the established trees. Average observed stem growth rate (per 10 cm *d* bins), expressed in carbon units(i.e. $\mathrm{kg\,C\,yr^{-1}}$), is compared with simulated $\Pi_{N,s}$ using the York method of best straight line, which holds when both *x* and *y* observations are subject to correlated errors that vary from point to point (York et al., 2004).

2.2.3 Permanent measurement (PM) sites

Inventory data from 40 RAINFOR permanent measurement plots (Fig. 2), including tree diameter and multiannual growth for all trees greater than 10 cm curated/managed in ForestPlots.net (Lopez-Gonzalez et al., 2009, 2011), are used to (a) validate the ability of the model to accurately simulate stand-level carbon fluxes and (b) explore patterns of Π_G, Π_N and $\mathrm{C_U}$ along the Amazonian climatic and soil fertility gradient. The size class distribution within each PM site is used to initialise the stand structure of the model and simulate patterns of productivity for the 2000–2006 period. Climate data for the same period were used here with the first year again used as a spin-up period (Sheffield et al., 2006). For those 40 PM plots, sample distributions of the traits quartet are available (Fyllas et al., 2009) as well as a description of soil chemical and physical properties (Quesada et al., 2011).

At the PM sites the simulated stand-level aboveground Π_N was compared with observed rates of aboveground growth (ΔB_ABG ($\mathrm{kg\,C\,m^{-2}\,yr^{-1}}$)) for trees that survived during the 2000–2006 time period using a SMA regression. A second step was to explore the way Π_G, Π_N and $\mathrm{C_U}$ vary across an Amazon climatic and soil fertility gradient (Quesada et al., 2010). The site scores of a principal components analysis (PCA) on the soil properties of the 40 PM plots (see Fyllas et al., 2009) are used to categorise plots along a fertility gradient (Φ_1), while the key climatic variables used were the annual mean temperature T_A and annual total precipitation P_A. A Kendall correlation coefficient (τ) was used to identify potential relationships of Π_G, Π_N and $\mathrm{C_U}$ with T_A, P_A and Φ_1, as in most cases non-linear associations were observed.

3 Results

3.1 Canopy conductance simulations at the EFM sites

Values of best model performance for g_0 and g_1 were different between sites, with g_0 = 0.035 ($\mathrm{mol\,m^{-2}\,s^{-1}}$) and g_1 = 7.5 at Caxiuanã, g_0 = 0.035 and g_1 = 7.0 at Manaus with g_0 = 0.01 and g_1 = 2.5 these being somewhat lower than the estimates of Domingues et al. (2013) at Tapajós. Simulated G_C was underestimated for Caxiuana ($\alpha = 0.85 \pm 0.05$) and Manaus ($\alpha = 0.90 \pm 0.02$), with the model overestimating G_C in Tapajos ($\alpha = 1.28 \pm 0.04$), but exhibiting an overall adequate performance (Fig. 3). For simulations at the IM and the PM sites, constant values of g_0 = 0.02 ($\mathrm{mol\,m^{-2}\,s^{-1}}$) and g_1 = 5 (–) were used, which are found within the range of values in the EFM sites and reported estimates (Medlyn et al., 2012; Domingues et al., 2013).

3.2 Stem growth rate simulations at the IM sites

The mean simulated stem growth rate $\Pi_{\mathrm{N,s}}$ of each tree in the seven IM plots was compared with the observed aboveground biomass gains (ΔB_{ABG}) for the 2000–2006 period. An accurate simulation of $\Pi_{\mathrm{N,s}}$ can be seen for small size classes, but with greater differences between the observed and the simulated multi-annual growth found for bigger trees (Fig. 4). At infertile ALP-30, the estimate slope of the York model indicated an overestimation of aboveground production ($\alpha = 1.18 \pm 0.06$), driven mainly by an overestimation of the mid-size classes. At BNT-04 the model underestimated the overall growth ($\alpha = 0.82 \pm 0.03$). Aboveground growth was overestimated in CAX-06 (1.11 ± 0.07). At TAP-55 ($\alpha = 1.44 \pm 0.15$) the model underestimated aboveground production (0.90 ± 0.06). At fertile AGP-01 ($\alpha = 1.36 \pm 0.08$) and AGP-02 ($\alpha = 1.25 \pm 0.05$) an overestimation of aboveground productivity was observed although with simulations of most size classes falling within the observed ranges. At TAM-05 ($\alpha = 0.79 \pm 0.07$) though, the simulated aboveground growth was underestimated with the overall slope driven by divergences in smaller size classes. The range and distribution of Π_N allocation to stem growth is adequately captured by TFS as summarised in Fig. S2.1.

3.3 GPP, NPP and CUE simulations at the PM sites

Simulated stand-level aboveground net primary productivity $\Pi_{N,A}$ was positively associated with observed changes in aboveground biomass of trees that survived in the PM plots over the 2000–2006 period ΔB_{ABG}, with an $R^2 = 0.42$, suggesting an adequate model behaviour (Fig. 5). A summary of simulated stand-level Π_G, Π_N and C_U relationships to key environmental drivers is given in Table 1 (see also Fig. S2.2). Π_G and Π_N and C_U were not associated with temperature. However all three measures of stand level productivity were positively related to annual precipitation and soil fertility.

4 Discussion

We have reported here on the core components of an individual-based model, developed in order to understand the patterns revealed by forest measurements across South America. In its current setup TFS does not explicitly simulate regeneration and mortality dynamics but rather uses the observed size distribution of trees at the study sites. The model is tailored to optimal exploitation of the RAINFOR type forest census, trait, and soil data. TFS is therefore able to take into account the structure of the stand and the functional trait variability identified along the main climatic and edaphic axes of the Amazon Basin. With the current setup we were able to reproduce the tree- and stand-level Π_N patterns found across Amazonia and to explore for potential environmental controls over stand-level Π_G, Π_N and C_U.

4.1 Scientific outcomes

Our simulations found no association of stand level *gross primary productivity* (Π_G) with temperature, probably due to the relatively small range of variation of temperature across our plots. Π_G decreased until an annual temperature of approximately 26 °C but remained relative constant above this point (Table 1, Fig. S2.2). However our simulations suggest that a strong association of Π_G with the annual precipitation and soil fertility of the plots. Π_G was positively related to annual precipitation over the entire range observed in the 40 PM plots. The association of Π_G with the fertility axis is in agreement with fertilisation experiments showing an increase with nutrient supply (Giardina et al., 2003). In our Basin-wide examination of Π_G the soil fertility and stand structure gradients are not however independent (Quesada et al., 2012), as in the RAINFOR network permanent plots it has been observed that bigger/older trees are more abundant on eastern infertile forests, where soil physical conditions can support a bigger tree size (Baker et al., 2009) with a lower risk of trees being uprooted (Chao et al., 2009). Bigger trees generally support a greater foliage area and thus could significantly contribute to the overall carbon assimilation of the stand. However bigger trees on infertile plots are generally characterised by lower leaf nutrient concentrations (Fyllas et al., 2009) and thus slower assimilation rates (Reich et al., 1994; Domingues et al., 2010). On the other hand a higher abundance of smaller trees with higher gas exchange rates is observed on more dynamic, fertile plots. Ultimately this indicates that stand structure should be specifically taken into account when simulating Π_G in tropical forests, and thus individual-based models could significantly contribute towards a deeper understanding of the functioning and sensitivity of these ecosystems.

In our simulations stand-level *net primary productivity* (Π_N) showed no significant association to annual temperature but increased with soil fertility and annual precipitation (Table 1, Fig. S2.2). Our Π_N simulations are in agreement with field observations of increasing aboveground wood productivity with precipitation (Quesada et al., 2012). Based on TFS parameterisation, photosynthetic rates are expected to be higher at fertile soil conditions due to higher leaf N and P concentration there (Fyllas et al., 2009; Domingues et al., 2010). Using a similar parameterisation for a "sun and shade" big leaf model, Mercado et al. (2011) found an increase in net canopy assimilation rate with leaf P content in agreement with our positive association between Π_N and soil fertility. Their simulated Π_G accounted for approximately 0.30 of the observed wood productivity in 33 study plots, and thus the $R^2 = 0.42$ between simulated Π_N and aboveground growth found here suggest a marginally improved model behaviour. It should be noted that our definition of soil fertility (Φ_1), based on the PCA analysis in Quesada et al. (2010), directly relates to soil P content. As shown first in the analysis of Quesada et al. (2012), where data from almost 60 plots were considered, aboveground Π_N is positively related to soil P content in lowland tropical forest. The increased Π_N in fertile environments (apart from the higher Π_G) seems to be enhanced by the greater abundance of small trees there. As tree size increases maintenance respiration "consumes" an increasing proportion of assimilated carbon, and thus at large size classes the proportion of trees which have enough carbon to allocate to growth decreases (Givnish, 1988; Cavaleri et al., 2008). This is in line with the negative relationship between coarse wood production and maximum height documented for some Amazonian trees (Baker et al., 2009).

In our simulations *carbon use efficiency* (C_U) ranged from 0.43 to 0.54. Recent research suggests that the C_U is not as constant as was previously assumed (De Lucia et al., 2007; Zhang et al., 2009). For example the meta-analysis of De Lucia et al. (2007) found that C_U varies from 0.23 to 0.83 in different forest types. Our average estimate of $C_U = 0.51$ is, however, above the range of reported in Malhi (2012). Zhang and colleagues (2009) identified a negative trend of the Π_N/Π_G ratio with temperature at the range of 20 to 30 °C, as also simulated here especially above 26 °C (Fig. S2.2). Simulated C_U increased with soil fertility, being marginally lower at infertile (0.48) compared to fertile (0.50) plots. This is attributable to smaller size class trees (with lower relative respiratory costs) constituting a greater proportion of the total stand biomass on the more fertile soils. One factor relating to soil fertility but not included in the current version is an implicit consideration of the costs of plant nutrient uptake (Lambers et al., 1983) either directly, or through other processes such as organic acid exudation (Jones et al., 2009) or the symbiotic associations (Duponnois et al., 2012).

One would expect these costs to be proportionally higher for stand of a low nutrient status, especially with regard to P (Quesada et al., 2012).

4.2 Practical implications

Modelling of tropical forests dynamics had traditionally aimed at a balance between simplicity, computational economy, and complexity. The enormous biological and biogeochemical heterogeneity of tropical forests (Townsend et al., 2008) places special importance on how modellers prioritise both the amount and the detail of processes that should be included to capture the main controls and feedbacks. On the other hand the finding that Amazonia is dominated by just 227 tree species (ter Steege et al., 2013) implies that most biogeochemical cycling in the world's largest tropical forest is performed by a tiny sliver of its diversity. Various types of tropical forest models have been published during the last decades. At the landscape level some approaches focus on realistically representing the light environment (Chave, 1999), while others emphasise on accurately grouping tree species and their response to environmental resources using field observations (Huth and Ditzer, 2000; Gourlet-Fleury and Houllier, 2000). At the continental scale one of the greatest uncertainties in the application of DGVMs arises from the way population dynamics are modelled (Delbart et al., 2010; Poulter et al., 2010). To deal with demographic processes not explicitly taken into account in DGVMs, Fisher et al. (2010) applied the ecosystem demography model after defining seven plant functional types characterised by strategies along a growth vs. survival dimension. Interestingly, by varying five parameters related to demographic processes, forest and biomass dynamics exhibited a wide range of responses to climate forcing.

Our study has aimed to balance the goal of model generality with that of model simplicity, and to draw on important recent lessons from field studies of the processes controlling Amazonian forest dynamics. We thus focus on accounting for the diversity in key functional traits, stand-structure, and their association with soil physical and chemical properties (Fyllas et al., 2009). Two modelling studies that follow a partly similar philosophy have recently been published. Scheiter and Higgins (2009) developed an individual-based DGVM where they also eschewed the functional group approach, but rather allowed for plants to allocate carbon as a function of the local environmental conditions. Falster and colleagues (2011) presented a trait-based modelling framework where they used leaf economic strategy, height, wood density and seed size to scale-up from individual scale processes to landscape predictions. Our approach nevertheless differs from these in the quantity of observational constraints used as we have endeavoured to constrain the simulations as much as possible with observational data in order to be able to explore the large-scale forest patterns revealed by the permanent plots measurement network.

Like all modelling efforts, TFS represents work in progress. We identify three particularly promising avenues for future improvements. Firstly, discrepancies between the observed and simulated stem level growth rates, particularly in larger size classes, could result from the allometric equations used to estimate aboveground biomass and growth not being species or size specific. The allometric equations used here express a generic height (H) vs. d relationship for Amazonia, without taking into account habitat and species differences, so a more accurate representation of tree architecture would probably result in better biomass growth estimation. Indeed, H–d relationships do vary significantly among species (King, 1996; Poorter et al., 2006) and across regions (Nogueira et al., 2008; Feldpausch et al., 2011; Goodman et al., 2013). An additional source of bias when estimating stem-level growth rates could be related to the uniform (static) allocation coefficient used in this study. For example, Litton et al. (2007) showed that allocation to aboveground tree biomass components increases with age and the availability of resources. Furthermore Castanho et al. (2013) improved the predictions of a DGVM by adjusting allocation coefficients based on soil texture. Such ontogenetic and/or resource based shifts in patterns of carbon allocation could be potentially modelled through the use of dynamic allocation schemes (Friedlingstein et al., 1999; Franklin et al., 2012).

The importance of realistically representing autotrophic respiration processes in models of vegetation dynamics is also highlighted here. Modelling respiration has proven to be a difficult task (Cannell and Thornley, 2000), and accurately representations of this component is of great importance for understanding the global C cycle (Valentini et al., 2000). For example the way respiration is represented in DGVMs could have a substantial control over the way the dynamics of Amazonian forest under scenarios of climatic change are simulated (Huntingford et al., 2004; Galbraith et al., 2010). Nitrogen content of plant tissue has been proven a good predictor of respiration rates (Reich et al., 2008). However Mori et al. (2010) suggested a mixed-power equation where the exponent varies from 1 to $3/4$ as size increases. Both the Reich and Mori models are implemented in TFS, but we found that a third method, combining the size and nitrogen control, performed better. Thus we suggest that an amalgamation of those two approaches could provide a better way to estimate respiration fluxes in the new generation of dynamic vegetation models. In addition leaf phosphorous content seems to constrain respiration rates stronger than nitrogen content in some tropical forests (Meir et al., 2001; Meir and Grace, 2002), and thus inclusion of this term in future equations of leaf respiration could increase their realism.

Finally, discrepancies in the observed vs. the simulated canopy conductance G_C could result from the parameterisation of the stomata conductance model of Medlyn et al. (2011). The estimates for g_0 and g_1 used in the 40 PM plots simulations were taken as constant. However Medlyn et al. (2011) suggested that g_0 and g_1 could vary with functional group. Thus the Amazon wide parameterisation used here should be replaced with local level estimates when appropriate gas exchange data are available, and ultimately with estimates based on linked functional traits as evidenced through recently documented associations between structural characteristics such as wood density and leaf area: sapwood ration with leaf physiological traits such as M_a and leaf $^{13}C/^{13}C$ ratio (Patino et al., 2012), although we also note that the extent of such structural/physiological linkages remains the subject of debate (Baraloto et al., 2010b). Alternative stomatal closure equations as a function of soil water availability (Harris et al., 2004) should also be tested along with the conductance model in future versions of the model.

5 Conclusions

We set out to develop a modelling framework for tropical forests that is relatively simple yet adequately complex to capture the main ecological gradients in the world's most extensive tropical forest. Our study places special emphasis on processes highlighted by recent field studies to strongly influence Amazonian forest dynamics, such as functional trait diversity and its association with multiple soil properties (Fyllas et al., 2009). In summary TFS is characterised by a relatively simple setup, which is capable to reproduce water and carbon fluxes as observed at both daily and multi-annual time scales. TFS represents an important link between inventory data, and large scale models with the incorporation of the continuum of plant strategies, through the inclusion of trait distributions providing a step towards better representing diversity in vegetation modelling (Lavorel et al., 2009), representing important processes and trait variation that cannot be adequately accounted for by a DGVM approach to vegetation modelling. Since TFS is based heavily on measured data, the model is well suited to testing hypotheses related to the present day Amazon biogeography and biogeochemical fluxes.

Code availability.

The JAVA source code can be obtained upon request. Contact: nfyllas@gmail.com.

Supplementary material related to this article is available online at http://www.geosci-model-dev-discuss.net/7/1413/2014/gmdd-7-1413-2014-supplement.pdf.

Acknowledgements. This research was supported by a Marie Curie Intra-European Fellowship within the 7th European Community Framework Programme to NM Fyllas. Manuel Gloor and Lina Mercado were funded by the AMAZONICA NERC consortium grant. OP is supported by an ERC Advanced Grant and a Royal Society Wolfson Research Merit Award. The work of

RAINFOR between 2000 and 2006 was supported primarily by the UK Natural Environment Research Council and the European Community Framework Programme through grants to OP, YM, and JL. Natalia Restrepo Coupe provided the gap filled Eddy Flux Tower data. Gabriela Lopez-Gonzalez and Sophie Fauset helped with data preparation. The Missouri Botanical Garden, Rodolfo Vasquez, Abel Monteagudo, Nigel Pitman, Adriana Prieto, Agustin Rudas, Natalino Silva, Chiqui Arroyo and Alejandro Araujo Murakami contributed permanent plot data to the RAINFOR network.

References

Aragão, L. E. O. C., Malhi, Y., Metcalfe, D. B., Silva-Espejo, J. E., Jiménez, E., Navarrete, D., Almeida, S., Costa, A. C. L., Salinas, N., Phillips, O. L., Anderson, L. O., Alvarez, E., Baker, T. R., Goncalvez, P. H., Huamán-Ovalle, J., Mamani-Solórzano, M., Meir, P., Monteagudo, A., Patiño, S., Peñuela, M. C., Prieto, A., Quesada, C. A., Rozas-Dávila, A., Rudas, A., Silva Jr., J. A., and Vásquez, R.: Above- and below-ground net primary productivity across ten Amazonian forests on contrasting soils, Biogeosciences, 6, 2759–2778, doi:10.5194/bg-6-2759-2009, 2009.

Baker, T. R., Phillips, O. L., Malhi, Y., Almeida, S., Arroyo, L., Di Fiore, A., Erwin, T., Higuchi, N., Killeen, T. J., and Laurance, S. G.: Increasing biomass in Amazonian forest plots, Philos. T. Roy. Soc. B, 359, 353–365, 2004.

Baker, T. R., Phillips, O. L., Laurance, W. F., Pitman, N. C. A., Almeida, S., Arroyo, L., DiFiore, A., Erwin, T., Higuchi, N., Killeen, T. J., Laurance, S. G., Nascimento, H., Monteagudo, A., Neill, D. A., Silva, J. N. M., Malhi, Y., López Gonzalez, G., Peacock, J., Quesada, C. A., Lewis, S. L., and Lloyd, J.: Do species traits determine patterns of wood production in Amazonian forests?, Biogeosciences, 6, 297–307, doi:10.5194/bg-6-297-2009, 2009.

Baraloto, C., Timothy Paine, C. E., Patino, S., Bonal, D., Herault, B., and Chave, J.: Functional trait variation and sampling strategies in species-rich plant communities, Funct. Ecol. 24, 208–216, 2010a.

Baraloto, C., Timothy Paine, C. E., Poorter, L., Beauchene, J., Bonal, D., Domenach, A.-M., Hérault, B., Patiño, S., Roggy, J.-C., and Chave, J.: Decoupled leaf and stem economics in rain forest trees, Ecol. Lett., 13, 1338–1347, 2010b.

Cannell, M. G. R. and Thornley, J. H. M.: Modelling the components of plant respiration: some guiding principles, Ann. Bot.-London, 85, 45–54, 2000.

Cavaleri, M. A., Oberbauer, S. F., and Ryan, M. G.: Foliar and ecosystem respiration in an old-growth tropical rain forest, Plant Cell Environ., 31, 473–483, 2008.

Chao, K.-J., Phillips, O. L., Monteagudo, A., Torres-Lezama, A., and Vásquez Martínez, R.: How do trees die? Mode of death in northern Amazonia, J. Veg. Sci., 20, 260–268, 2009.

Chave, J.: Study of structural, successional and spatial patterns in tropical rain forests using TROLL, a spatially explicit forest model, Ecol. Model., 124, 233–254, 1999.

Chave, J., Andalo, C., Brown, S., Cairns, M. A., Chambers, J. Q., Eamus, D., Fölster, H., Fromard, F., Higuchi, N., and Kira, T.: Tree allometry and improved estimation of carbon stocks and balance in tropical forests, Oecologia, 145, 87–99, 2005.

Chave, J., Coomes, D., Jansen, S., Lewis, S. L., Swenson, N. G., and Zanne, A. E.: Towards a worldwide wood economics spectrum, Ecol. Lett., 12, 351–366, 2009.

Clark, D. B., Mercado, L. M., Sitch, S., Jones, C. D., Gedney, N., Best, M. J., Pryor, M., Rooney, G. G., Essery, R. L. H., Blyth, E., Boucher, O., Harding, R. J., Huntingford, C., and Cox, P. M.: The Joint UK Land Environment Simulator (JULES), model description – Part 2: Carbon fluxes and vegetation dynamics, Geosci. Model Dev., 4, 701–722, doi:10.5194/gmd-4-701-2011, 2011.

Cox, P. M., Betts, R. A., Collins, M., Harris, P. P., Huntingford, C., and Jones, C. D.: Amazonian forest dieback under climate-carbon cycle projections for the 21st century, Theor. Appl. Climatol., 78, 137–156, 2004.

Cramer, W., Bondeau, A., Schaphoff, S., Lucht, W., Smith, B., and Sitch, S.: Tropical forests and the global carbon cycle: impacts of atmospheric carbon dioxide, climate change and rate of deforestation, Philos. T. R. Soc. B, 359, 331–343, 2004.

Delbart, N., Ciais, P., Chave, J., Viovy, N., Malhi, Y., and Le Toan, T.: Mortality as a key driver of the spatial distribution of aboveground biomass in Amazonian forest: results from a dynamic vegetation model, Biogeosciences, 7, 3027–3039, doi:10.5194/bg-7-3027-2010, 2010.

DeLucia, E., Drake, J. E., Thomas, R. B., and Gonzalez-Meller, M.: Forest carbon use efficiency: is respiration a constant fraction of gross primary production?, Glob. Change Biol., 13, 1157–1167, 2007.

Domingues, T. F., Meir, P., Feldpausch, T. R., Saiz, G., Veenendaal, E. M., Schrodt, F., Bird, M., Djagbletey, G., Hien, F., and Compaore, H.: Co-limitation of photosynthetic capacity by nitrogen and phosphorus in West Africa woodlands, Plant Cell Environ., 33, 959–980, 2010.

Domingues, T. F., Martinelli, L. A., and Ehleringer, J. R.: Seasonal patterns of leaf-level photosynthetic gas exchange in an eastern Amazonian rain forest, Plant Ecol. Div., 7, 189–203, 2013.

Duponnois, R., Baudoin, E., Thioulouse, J., Hafidi, M., Galiana, A., Lebrun, M., and Prin, Y.: The impact of mycorrhizosphere bacterial communities on soil biofunctioning in tropical and mediterranean forest ecosystems, in: Bacteria in Agrobiology: Plant Probiotics, edited by: Maheshwari, D. K., Springer, Berlin Heidelberg, 79–95, 2012.

Falster, D. S., Brännström, Å., Dieckmann, U., and Westoby, M.: Influence of four major plant traits on average height, leaf-area cover, net primary productivity, and biomass density in single-species forests: a theoretical investigation, J. Ecol., 99, 148–164, 2011.

Farquhar, G. D., von Caemmerer, S., and Berry, J. A.: A biochemical model of photosynthetic CO_2 assimilation in leaves of C3 species, Planta, 149, 78–90, 1980.

Feldpausch, T. R., Banin, L., Phillips, O. L., Baker, T. R., Lewis, S. L., Quesada, C. A., Affum-Baffoe, K., Arets, E. J. M. M., Berry, N. J., Bird, M., Brondizio, E. S., de Camargo, P., Chave, J., Djagbletey, G., Domingues, T. F., Drescher, M., Fearnside, P. M., França, M. B., Fyllas, N. M., Lopez-Gonzalez, G., Hladik, A., Higuchi, N., Hunter, M. O., Iida, Y., Salim, K. A., Kassim, A. R., Keller, M., Kemp, J., King, D. A., Lovett, J. C., Marimon, B. S., Marimon-Junior, B. H., Lenza, E., Marshall, A. R., Metcalfe, D. J., Mitchard, E. T. A., Moran, E. F., Nelson, B. W., Nilus, R., Nogueira, E. M., Palace, M., Patiño, S., Peh, K. S.-H., Raventos, M. T., Reitsma, J. M., Saiz, G., Schrodt, F., Sonké, B., Taedoumg, H. E., Tan, S., White, L., Wöll, H., and Lloyd, J.: Height-diameter allometry of tropical forest trees, Biogeosciences, 8, 1081–1106, doi:10.5194/bg-8-1081-2011, 2011.

Fisher, R., McDowell, N., Purves, D., Moorcroft, P., Sitch, S., Cox, P., Huntingford, C., Meir, P., and Ian Woodward, F.: Assessing uncertainties in a second-generation dynamic vegetation model caused by ecological scale limitations, New Phytol., 187, 666–681, 2010.

Franklin, O., Johansson, J., Dewar, R. C., Dieckmann, U., McMurtrie, R. E., Brännström, Å., and Dybzinski, R.: Modeling carbon allocation in trees: a search for principles, Tree Physiol., 32, 648–666, 2012.

Fyllas, N. M., Patiño, S., Baker, T. R., Bielefeld Nardoto, G., Martinelli, L. A., Quesada, C. A., Paiva, R., Schwarz, M., Horna, V., Mercado, L. M., Santos, A., Arroyo, L., Jiménez, E. M., Luizão, F. J., Neill, D. A., Silva, N., Prieto, A., Rudas, A., Silviera, M., Vieira, I. C. G., Lopez-Gonzalez, G., Malhi, Y., Phillips, O. L., and Lloyd, J.: Basin-wide variations in foliar properties of Amazonian forest: phylogeny, soils and climate, Biogeosciences, 6, 2677–2708, doi:10.5194/bg-6-2677-2009, 2009.

Fyllas, N. M., Quesada, C. A., and Lloyd, J.: Deriving plant functional types for Amazonian forests for use in vegetation dynamics models, Perspect. Plant Ecol., 14, 97–110, 2012.

Galbraith, D., Levy, P. E., Sitch, S., Huntingford, C., Cox, P., Williams, M., and Meir, P.: Multiple mechanisms of Amazonian forest biomass losses in three dynamic global vegetation models under climate change, New Phytol., 187, 647–665, 2010.

Giardina, C. P., Ryan, M. G., Binkley, D., and Fownes, J. H.: Primary production and carbon allocation in relation to nutrient supply in a tropical experimental forest, Glob. Change Biol., 9, 1438–1450, 2003.

Gloor, M., Brienen, R. J. W., Galbraith, D., Feldpausch, T. R., Schöngart, J., Guyot, J.-L., Espinoza, J. C., Lloyd, J., and Phillips, O. L.: Intensification of the Amazon hydrological cycle over the last two decades, Geophys. Res. Lett., 40, 1729–1733, 2013.

Goodman, R. C., Phillips, O. L., and Baker, T. R.: The importance of crown dimensions to improve tropical tree biomass estimates, Ecol. Appl., online first, doi:10.1890/13-0070.1, 2013.

Gourlet-Fleury, S. and Houllier, F.: Modelling diameter increment in a lowland evergreen rain forest in French Guiana, Forest Ecol. Manag., 131, 269–289, 2000.

Gower, S. T., McMurtrie, R. E., and Murty, D.: Aboveground net primary production decline with stand age: potential causes, Trends Ecol. Evol., 11, 378–382, 1996.

Harris, P. P., Huntingford, C., Cox, P. M., Gash, J. H., and Malhi, Y.: Effect of soil moisture on canopy conductance of Amazonian rainforest, Agr. Forest Meteorol., 122, 215–227, 2004.

Higgins, M. A., Ruokolainen, K., Tuomisto, H., Llerena, N., Cardenas, G., Phillips, O. L., Vásquez, R., and Räsänen, M.: Geological control of floristic composition in Amazonian forests, J. Biogeogr., 38, 2136–2149, 2011.

Hodnett, M. G. and Tomasella, J.: Marked differences between van Genuchten soil water-retention parameters for temperate and tropical soils: a new water-retention pedo-transfer functions developed for tropical soils, Geoderma, 108, 155–180, 2002.

Huntingford, C., Harris, P. P., Gedney, N., Cox, P. M., Betts, R. A., Marengo, J. A., and Gash, J. H. C.: Using a GCM analogue model to investigate the potential for Amazonian forest dieback, Theor. Appl. Climatol., 78, 177–185, 2004.

Huntingford, C., Zelazowski, P., Galbraith, D., Mercado, L. M., Sitch, S., Fisher, R., Lomas, M., Walker, A. P., Jones, C. D., Booth, B. B. B., Malhi, Y., Hemming, D., Kay, G., Good, P., Lewis, S. L., Phillips, O. L., Atkin, O. K., Lloyd, J., Gloor, E., Zaragoza-Castells, J., Meir, P., Betts, R., Harris, P. P., Nobre, C., Marengo, J., and Cox, P. M.: Simulated resilience of tropical rainforests to CO_2-induced climate change, Nat. Geosci., 6, 268–273, 2013.

Huth, A. and Ditzer, T.: Simulation of the growth of a lowland Dipterocarp rain forest with FORMIX3, Ecol. Model., 134, 1–25, 2000.

Jones, D. L., Nguyen, C., and Finlay, R. D.: Carbon flow in the rhizosphere: carbon trading at the soil–root interface, Plant Soil, 321, 5–33, 2009.

Keeling, H. C., Baker, T. R., Martinez, R. V., Monteagudo, A., and Phillips, O. L.: Contrasting patterns of diameter and biomass increment across tree functional groups in Amazonian forests, Oecologia, 158, 521–534, 2008.

King, D. A.: Allometry and life history of tropical trees, J. Trop. Ecol., 12, 25–44, 1996.

Larjavaara, M. and Muller-Landau, H. C.: Still rethinking the value of high wood density, Am. J. Bot., 99, 165–168, 2012.

Lavorel, S., Díaz, S., Cornelissen, J. H. C., Garnier, E., Harrison, S. P., McIntyre, S., Pausas, J. G., Pérez-Harguindeguy, N., Roumet, C., and Urcelay, C.: Plant functional types: are we getting any closer to the Holy Grail?, in: Terrestrial Ecosystems in a Changing World, Springer, 149–164, 2007.

Lewis, S. L., Phillips, O. L., Baker, T. R., Lloyd, J., Malhi, Y., Almeida, S., Higuchi, N., Laurance, W. F., Neill, D. A., and Silva, J. N. M.: Concerted changes in tropical forest structure and dynamics: evidence from 50 South American long-term plots, Philos. T. R. Soc. B, 359, 421–436, 2004.

Litton, C. M., Raich, J. W., and Ryan, M. G.: Carbon allocation in forest ecosystems, Glob. Change Biol., 13, 2089–2109, 2007.

Lloyd, J., Patiño, S., Paiva, R. Q., Nardoto, G. B., Quesada, C. A., Santos, A. J. B., Baker, T. R., Brand, W. A., Hilke, I., Gielmann, H., Raessler, M., Luizão, F. J., Martinelli, L. A., and Mercado, L. M.: Optimisation of photosynthetic carbon gain and within-canopy gradients of associated foliar traits for Amazon forest trees, Biogeosciences, 7, 1833–1859, doi:10.5194/bg-7-1833-2010, 2010.

Lopez-Gonzalez, G., Lewis, S. L., Burkitt, M., and Phillips, O. L.: ForestPlots.net: a web application and research tool to manage and analyse tropical forest plot data, J. Veg. Sci., 22, 610–613, 2011.

Lopez-Gonzalez, G., Lewis, S. L., Burkitt, M., Baker, T. R., and Phillips, O. L.: ForestPlots.net Database, available at: www.forestplots.net (last access: 10 September 2013), 2013.

Malhi, Y.: The carbon balance of tropical forest regions, 1990–2005, Current Opinion in Environmental Sustainability, 2, 237–244, 2010.

Malhi, Y.: The productivity, metabolism and carbon cycle of tropical forest vegetation, J. Ecol., 100, 65–75, 2012.

Malhi, Y. and Wright, J.: Spatial patterns and recent trends in the climate of tropical rainforest regions, Philos. T. R. Soc. B, 359, 311–329, 2004.

Malhi, Y., Phillips, O. L., Lloyd, J., Baker, T., Wright, J., Almeida, S., Arroyo, L., Frederiksen, T., Grace, J., and Higuchi, N.: An international network to monitor the structure, composition and dynamics of Amazonian forests (RAINFOR), J. Veg. Sci., 13, 439–450, 2002.

Malhi, Y., Wood, D., Baker, T. R., Wright, J., Phillips, O. L., Cochrane, T., Meir, P., Chave, J., Almeida, S., and Arroyo, L.: The regional variation of aboveground live biomass in old-growth Amazonian forests, Glob. Change Biol., 12, 1107–1138, 2006.

Malhi, Y., Doughty, C., and Galbraith, D.: The allocation of ecosystem net primary productivity in tropical forests, Philos. T. R. Soc. B, 366, 3225–3245, 2011.

Medlyn, B. E., Duursma, R. A., Eamus, D., Ellsworth, D. S., Prentice, I. C., Barton, C. V., Crous, K. Y., de Angelis, P., Freeman, M., and Wingate, L.: Reconciling the optimal and empirical approaches to modelling stomatal conductance, Glob. Change Biol., 17, 2134–2144, 2011.

Medlyn, B. E., Duursma, R. A., Eamus, D., Ellsworth, D. S., Colin Prentice, I., Barton, C. V., Crous, K. Y., Angelis, P., Freeman, M., and Wingate, L.: Reconciling the optimal and empirical approaches to modelling stomatal conductance, Glob. Change Biol., 18, 3476–3476, 2012.

Mercado, L. M., Patiño, S., Domingues, T. F., Fyllas, N. M., Weedon, G. P., Sitch, S., Quesada, C. A., Phillips, O. L., Aragão, L. E., and Malhi, Y.: Variations in Amazon forest productivity correlated with foliar nutrients and modelled rates of photosynthetic carbon supply, Philos. T. R. Soc. B, 366, 3316–3329, 2011.

Moorcroft, P. R., Hurtt, G. C., and Pacala, S. W.: A method for scaling vegetation dynamics: the ecosystem demography model (ED), Ecol. Monogr., 71, 557–586, 2001.

Mori, S., Yamaji, K., Ishida, A., Prokushkin, S. G., Masyagina, O. V., Hagihara, A., Hoque, A. R., Suwa, R., Osawa, A., and Nishizono, T.: Mixed-power scaling of whole-plant respiration from seedlings to giant trees, P. Natl. Acad. Sci. USA, 107, 1447–1451, 2010.

Nogueira, E. M., Fearnside, P. M., Nelson, B. W., Barbosa, R. I., and Keizer, E. W. H.: Estimates of forest biomass in the Brazilian Amazon: new allometric equations and adjustments to biomass from wood-volume inventories, Forest Ecol. Manag., 256, 1853–1867, 2008.

Patiño, S., Lloyd, J., Paiva, R., Baker, T. R., Quesada, C. A., Mercado, L. M., Schmerler, J., Schwarz, M., Santos, A. J. B., Aguilar, A., Czimczik, C. I., Gallo, J., Horna, V., Hoyos, E. J., Jimenez, E. M., Palomino, W., Peacock, J., Peña-Cruz, A., Sarmiento, C., Sota, A., Turriago, J. D., Villanueva, B., Vitzthum, P., Alvarez, E., Arroyo, L., Baraloto, C., Bonal, D., Chave, J., Costa, A. C. L., Herrera, R., Higuchi, N., Killeen, T., Leal, E., Luizão, F., Meir, P., Monteagudo, A., Neil, D., Núñez-Vargas, P., Peñuela, M. C., Pitman, N., Priante Filho, N., Prieto, A., Panfil, S. N., Rudas, A., Salomão, R., Silva, N., Silveira, M., Soares deAlmeida, S., Torres-Lezama, A., Vásquez-Martínez, R., Vieira, I., Malhi, Y., and Phillips, O. L.: Branch xylem density variations across the Amazon Basin, Biogeosciences, 6, 545–568, doi:10.5194/bg-6-545-2009, 2009.

Patiño, S., Fyllas, N. M., Baker, T. R., Paiva, R., Quesada, C. A., Santos, A. J. B., Schwarz, M., ter Steege, H., Phillips, O. L., and Lloyd, J.: Coordination of physiological and structural traits in Amazon forest trees, Biogeosciences, 9, 775–801, doi:10.5194/bg-9-775-2012, 2012.

Phillips, O. L., Malhi, Y., Higuchi, N., Laurance, W. F., Núnez, P. V., Vásquez, R. M., Laurance, S. G., Ferreira, L. V., Stern, M., and Brown, S.: Changes in the carbon balance of tropical forests: evidence from long-term plots, Science, 282, 439–442, 1998.

Phillips, O. L., Baker, T. R., Arroyo, L., Higuchi, N., Killeen, T. J., Laurance, W. F., Lewis, S. L., Lloyd, J., Malhi, Y., and Monteagudo, A.: Pattern and process in Amazon tree turnover, 1976–2001, Philos. T. R. Soc. B, 359, 381–407, 2004.

Phillips, O. L., Aragão, L. E., Lewis, S. L., Fisher, J. B., Lloyd, J., López-González, G., Malhi, Y., Monteagudo, A., Peacock, J., and Quesada, C. A.: Drought sensitivity of the Amazon rainforest, Science, 323, 1344–1347, 2009.

Poulter, B., Aragao, L., Heyder, U., Gumpenberger, M., Heinke, J., Langerwisch, F., Rammig, A., Thonicke, K., and Cramer, W.: Net biome production of the Amazon Basin in the 21st century, Glob. Change Biol., 16, 2062–2075, 2010.

Purves, D. W., Lichstein, J. W., and Pacala, S. W.: Crown plasticity and competition for canopy space: a new spatially implicit model parameterized for 250 North American tree species, PLoS One, 2, e870, doi:10.1371/journal.pone.0000870, 2007.

Pury, D. de and Farquhar, G. D.: Simple scaling of photosynthesis from leaves to canopies without the errors of big-leaf models, Plant Cell Environ., 20, 537–557, 1997.

Quesada, C. A., Lloyd, J., Schwarz, M., Patiño, S., Baker, T. R., Czimczik, C., Fyllas, N. M., Martinelli, L., Nardoto, G. B., Schmerler, J., Santos, A. J. B., Hodnett, M. G., Herrera, R., Luizão, F. J., Arneth, A., Lloyd, G., Dezzeo, N., Hilke, I., Kuhlmann, I., Raessler, M., Brand, W. A., Geilmann, H., Moraes Filho, J. O., Carvalho, F. P., Araujo Filho, R. N., Chaves, J. E., Cruz Junior, O. F., Pimentel, T. P., and Paiva, R.: Variations in chemical and physical properties of Amazon forest soils in relation to their genesis, Biogeosciences, 7, 1515–1541, doi:10.5194/bg-7-1515-2010, 2010.

Quesada, C. A., Lloyd, J., Anderson, L. O., Fyllas, N. M., Schwarz, M., and Czimczik, C. I.: Soils of Amazonia with particular reference to the RAINFOR sites, Biogeosciences, 8, 1415–1440, doi:10.5194/bg-8-1415-2011, 2011.

Quesada, C. A., Phillips, O. L., Schwarz, M., Czimczik, C. I., Baker, T. R., Patiño, S., Fyllas, N. M., Hodnett, M. G., Herrera, R., Almeida, S., Alvarez Dávila, E., Arneth, A., Arroyo, L., Chao, K. J., Dezzeo, N., Erwin, T., di Fiore, A., Higuchi, N., Honorio Coronado, E., Jimenez, E. M., Killeen, T., Lezama, A. T., Lloyd, G., López-González, G., Luizão, F. J., Malhi, Y., Monteagudo, A., Neill, D. A., Núñez Vargas, P., Paiva, R., Peacock, J., Peñuela, M. C., Peña Cruz, A., Pitman, N., Priante Filho, N., Prieto, A., Ramírez, H., Rudas, A., Salomão, R., Santos, A. J. B., Schmerler, J., Silva, N., Silveira, M., Vásquez, R., Vieira, I., Terborgh, J., and Lloyd, J.: Basin-wide variations in Amazon forest structure and function are mediated by both soils and climate, Biogeosciences, 9, 2203–2246, doi:10.5194/bg-9-2203-2012, 2012.

Raaimakers, D., Boot, R. G. A., Dijkstra, P., and Pot, S.: Photosynthetic rates in relation to leaf phosphorus content in pioneer versus climax tropical rainforest trees, Oecologia, 102, 120–125, 1995.

Reich, P. B., Walters, M. B., Ellsworth, D. S., and Uhl, C.: Photosynthesis–nitrogen relations in Amazonian tree species, Oecologia, 97, 62–72, 1994.

Reich, P. B., Walters, M. B., and Ellsworth, D. S.: From tropics to tundra: global convergence in plant functioning, P. Natl. Acad. Sci. USA, 94, 13730–13734, 1997.

Reich, P. B., Tjoelker, M. G., Pregitzer, K. S., Wright, I. J., Oleksyn, J., and Machado, J.-L.: Scaling of respiration to nitrogen in leaves, stems and roots of higher land plants, Ecol. Lett., 11, 793–801, 2008.

Reich, P. B., Oleksyn, J., and Wright, I. J.: Leaf phosphorus influences the photosynthesis–nitrogen relation: a cross-biome analysis of 314 species, Oecologia, 160, 207–212, 2009.

Scheiter, S. and Higgins, S. I.: Impacts of climate change on the vegetation of Africa: an adaptive dynamic vegetation modelling approach, Glob. Change Biol., 15, 2224–2246, 2009.

Sheffield, J., Goteti, G., and Wood, E. F.: Development of a 50-year high-resolution global dataset of meteorological forcings for land surface modeling, J. Climate, 19, 3088–3111, 2006.

Shukla, J., Nobre, C., and Sellers, P.: Amazon deforestation and climate change, Science, 247, 1322–1325, 1990.

Sitch, S., Smith, B., Prentice, I. C., Arneth, A., Bondeau, A., Cramer, W., Kaplan, J. O., Levis, S., Lucht, W., and Sykes, M. T.: Evaluation of ecosystem dynamics, plant geography and terrestrial carbon cycling in the LPJ dynamic global vegetation model, Glob. Change Biol., 9, 161–185, 2003.

Sombroek, W.: Amazon landforms and soils in relation to biological diversity, Acta Amazonica, 30, 81–100, 2000.

Sombroek, W.: Spatial and temporal patterns of Amazon rainfall: consequences for the planning of agricultural occupation and the protection of primary forests, AMBIO: A Journal of the Human Environment, 30, 388–396, 2001.

Spracklen, D. V., Arnold, S. R., and Taylor, C. M.: Observations of increased tropical rainfall preceded by air passage over forests, Nature, 489, 282–285, 2012.

Sultan, S. E.: Phenotypic plasticity for plant development, function and life history, Trends Plant Sci., 5, 537–542, 2000.

Taylor, M. S. and Thompson, J. R.: A data based algorithm for the generation of random vectors, Comput. Stat. Data An., 4, 93–101, 1986.

Ter Steege, H., Pitman, N. C., Phillips, O. L., Chave, J., Sabatier, D., Duque, A., Molino, J.-F., Prévost, M.-F., Spichiger, R., and Castellanos, H.: Continental-scale patterns of canopy tree composition and function across Amazonia, Nature, 443, 444–447, 2006.

Ter Steege, H., Pitman, N. C., Sabatier, D., Baraloto, C., Salomão, R. P., Guevara, J. E., Phillips, O. L., Castilho, C. V., Magnusson, W. E., and Molino, J.-F.: Hyperdominance in the Amazonian tree flora, Science, 342, 1243092, doi:10.1126/science.1243092, 2013.

Tjoelker, M. G., Oleksyn, J., and Reich, P. B.: Modelling respiration of vegetation: evidence for a general temperature-dependent Q10, Glob. Change Biol., 7, 223–230, 2001.

Townsend, A. R., Asner, G. P., and Cleveland, C. C.: The biogeochemical heterogeneity of tropical forests, Trends Ecol. Evol., 23, 424–431, 2008.

Valentini, R., Matteucci, G., Dolman, A. J., Schulze, E.-D., Rebmann, C., Moors, E. J., Granier, A., Gross, P., Jensen, N. O., and Pilegaard, K.: Respiration as the main determinant of carbon balance in European forests, Nature, 404, 861–865, 2000.

Van Genuchten, M. T.: A closed-form equation for predicting the hydraulic conductivity of unsaturated soils, Soil Sci. Soc. Am. J., 44, 892–898, 1980.

Vitousek, P. M. and Farrington, H.: Nutrient limitation and soil development: experimental test of a biogeochemical theory, Biogeochemistry, 37, 63–75, 1997.

Walker, T. W. and Syers, J. K.: The fate of phosphorus during pedogenesis, Geoderma, 15, 1–19, 1976.

Wang, Y.-P. and Leuning, R.: A two-leaf model for canopy conductance, photosynthesis and partitioning of available energy I: Model description and comparison with a multi-layered model, Agr. Forest Meteorol., 91, 89–111, 1998.

White, A., Cannell, M. G., and Friend, A. D.: Climate change impacts on ecosystems and the terrestrial carbon sink: a new assessment, Global Environ. Chang., 9, 21–30, 1999.

Wright, I. J., Reich, P. B., Westoby, M., Ackerly, D. D., Baruch, Z., Bongers, F., Cavender-Bares, J., Chapin, T., Cornelissen, J. H., and Diemer, M.: The worldwide leaf economics spectrum, Nature, 428, 821–827, 2004.

York, D., Evensen, N. M., Martínez, M. L., and Delgado, J. D. B.: Unified equations for the slope, intercept, and standard errors of the best straight line, Am. J. Phys., 72, 367–375, 2004.

Zhang, Y., Xu, M., Chen, H., and Adams, J.: Global pattern of NPP to GPP ratio derived from MODIS data: effects of ecosystem type, geographical location and climate, Global. Ecol. Biogeogr., 18, 280–290, 2009.

Table 1. Kendall correlation coefficients (τ) and associated significance levels (p) between simulated Π_G, Π_N and C_U and key environmental factors.

	Π_G (kg C m^{-2} yr^{-1})	Π_N (kg C m^{-2} yr^{-1})	C_U (–)
Mean Annual Temperature – T_A (°C)	$\tau = -0.17$ $p = 0.131$	$\tau = -0.21$ $p = 0.065$	$\tau = -0.11$ $p = 0.33$
Total Annual Precipitation – P_A (mm)	$\tau = 0.54$ $p < 0.001$	$\tau = 0.60$ $p < 0.001$	$\tau = 0.36$ $p = 0.002$
Soil Fertility – Φ1 (PCA Axis 1)	$\tau = 0.48$ $p < 0.001$	$\tau = 0.50$ $p < 0.001$	$\tau = 0.39$ $p < 0.001$

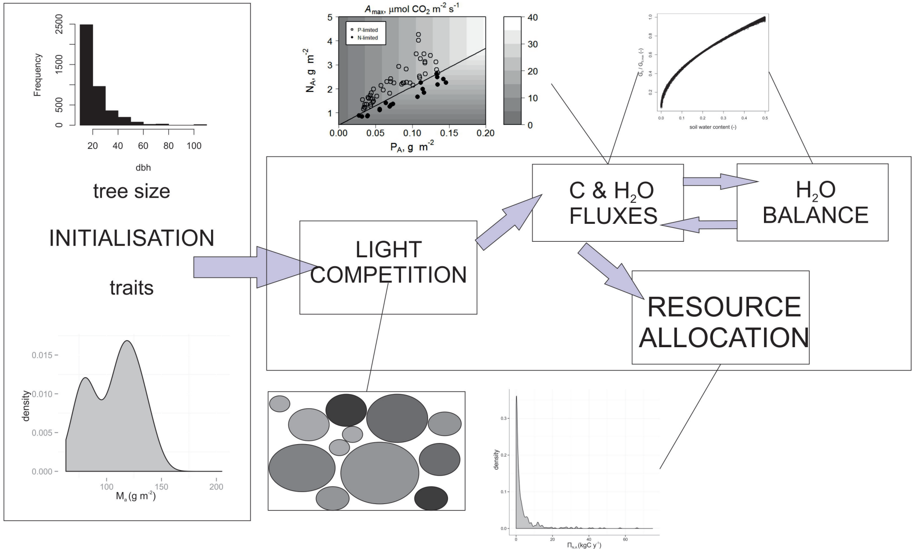

Fig. 1. The five basic components of the model and information flow among them. Tree by tree traits and size initialisation takes place at the beginning of each simulation. Carbon and water fluxes, as well as gross and net primary productivity are estimated daily.

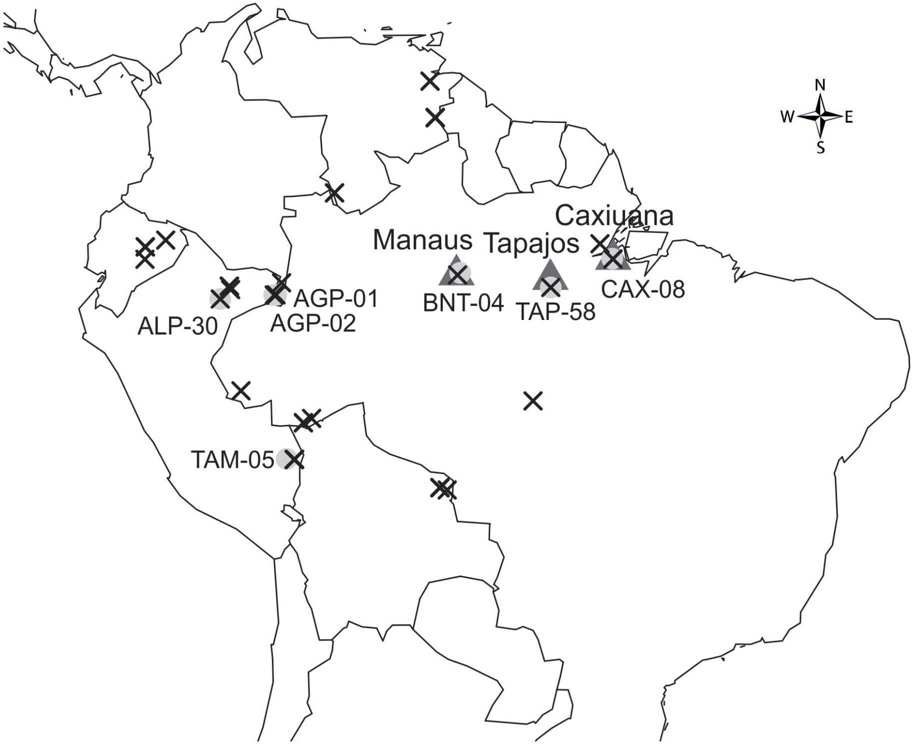

Fig. 2. Geographic distribution of study sites. Dark grey triangles indicate the three eddy flux tower sites (with local names), light gray circles indicate the seven intensive measurement plots (with plot codes), and crosses indicate the coordinates of the 40 RAINFOR permanent measurement plots.

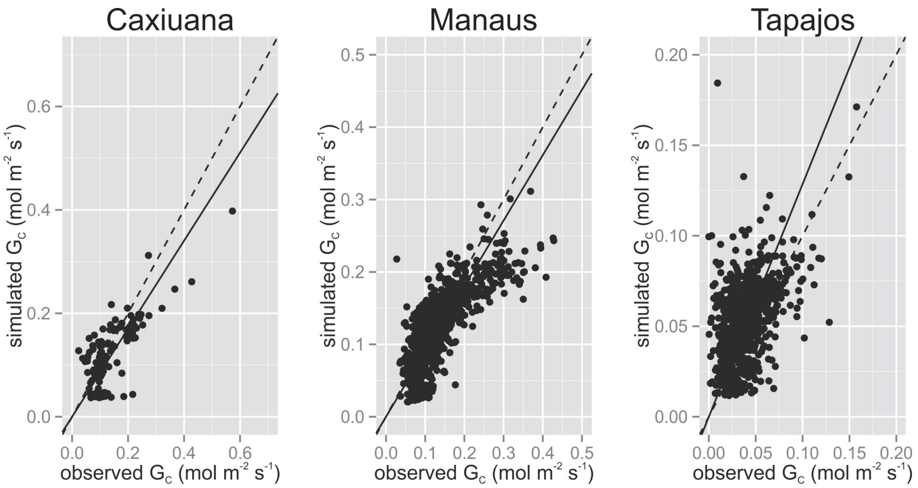

Fig. 3. Simulated against observed mean daily canopy conductance G_C for the three sites with eddy flux data. The broken line represents an 1 : 1 relationship and the continuous line illustrates a standardised major axis (SMA) regression.

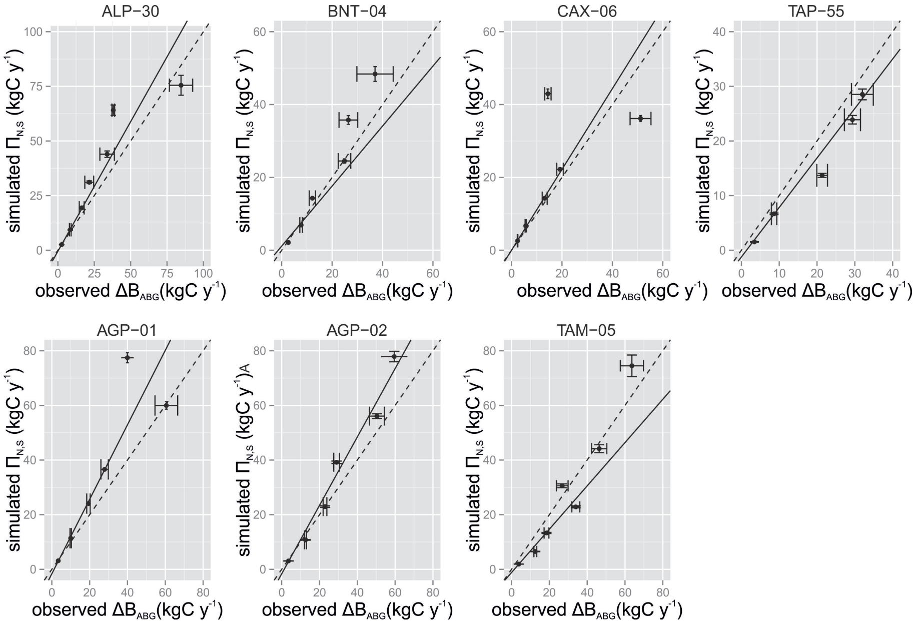

Fig. 4. Simulated stem growth rate $\Pi_{N,s}$ against observed aboveground biomass change ΔB_{ABG} for different size classes for the 2000–2006 period. Upper panel groups together infertile plots, with fertile plots found at the lower panel. The broken line represents an 1 : 1 relationship continuous. The continuous line illustrates the straight line fit using the York method (see text for details).

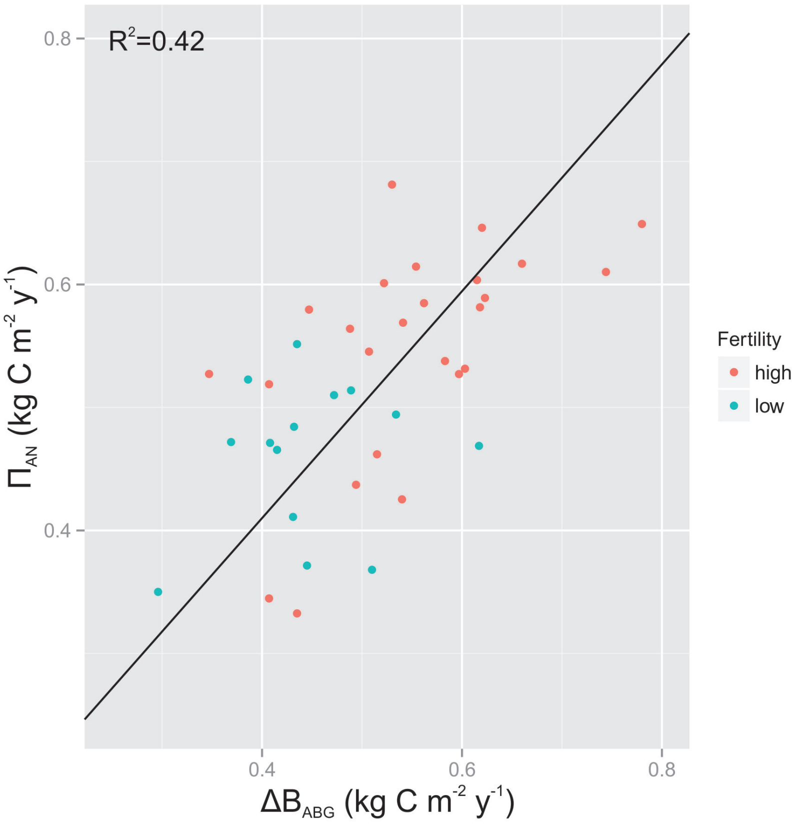

Fig. 5. Simulated stand-level aboveground net primary productivity (Π_{AN}) against observed stand-level aboveground biomass growth (ΔB_{ABG}) of surviving trees, at the 40 PM plots. The line illustrates a SMA regression of $\alpha = 0.92$ (0.72 … 1.18) and $R^2 = 0.42$. Red dots indicate high fertility and blue dots indicate low fertility plots.